Remediation of multilayer soils contaminated by heavy chlorinated solvents using biopolymer-surfactant mixtures: Two-dimensional flow experiments and simulations

Amir Alamooti [a,b,c,d,*], Stéfan Colombano [a], Zakari Abdullaziz Glabe [a], Fabien Lion [a], Dorian Davarzani [a], Azita Ahmadi-Sénichault [b,c]

[a] *BRGM (French Geological Survey), Orléans 45060, France*
[b] *University of Bordeaux, CNRS, Bordeaux INP, I2M, UMR 5295, F-33400 Talence, France*
[c] *Arts et Metiers Institute of Technology, CNRS, Bordeaux INP, Hesam Universite, I2M, UMR 5295, F-33400 Talence, France*
[d] *ADEME (French Environment and Energy Management Agency), Angers 49004, France*

ABSTRACT

To assess the efficiency of remediating dense non-aqueous phase liquids (DNAPLs), here heavy chlorinated solvents, through injection of xanthan solutions with or without surfactant (sodium dodecylbenzenesulfonate: SDBS), we conducted a comprehensive investigation involving rheological measurements, column (1D) and two-dimensional (2D) sandbox experiments, as well as numerical simulations on two-layers sand packs. Sand packs with grain sizes of 0.2–0.3 mm and 0.4–0.6 mm, chosen to represent the low and high permeable soil layers respectively, were selected to be representative of real polluted field. The rheological analysis of xanthan solutions showed that the addition of SDBS to the solution reduced its viscosity due to repulsive electrostatic forces and hydrophobic interactions between the molecules while preserving its shear-thinning behavior. Results of two-phase flow experiments depicted that adding SDBS to the polymer solution led to a reduced differential pressure along the soil and improvements of the DNAPL recovery factor of approximately 0.15 and 0.07 in 1D homogeneous and 2D layered systems, respectively. 2D experiments revealed that the displacement of DNAPL in multilayer zones was affected by permeability difference and density contrast in a heterogeneous soil. Simulation of multiphase flow in a multilayered system was performed by incorporating non-Newtonian properties and coupling the continuity equation with generalized Darcy's law. The results of modeling and experiments are very consistent. Numerical simulations showed that for an unconfined soil, the recovery of DNAPL by injection of xanthan solution can be reduced for more than 50%. In a large 2D experimental system, the combination of injecting xanthan with blocking the contaminated zone led to a promising remediation of DNAPL-contaminated layered zones, with a recovery of 0.87.

1. Introduction

Polymer injection is being used as an effective soil/groundwater remediation technology (Alamooti et al., 2022; Bouzid and Fatin-Rouge, 2022; Martel et al., 1998). Polymer flushing has several advantages over other advanced soil remediation technologies such as surfactant flushing (Lee et al., 2005; Pennell and Abriola, 2017; Walker et al., 2022) or foam injection (Liao et al., 2021; Omirbekov et al., 2020). Polymer solutions by increasing fluid viscosity, can enhance pollutant recovery, and stabilize the displacement front, minimize channeling,

and aid in better control and containment during soil remediation. Shear thinning polymers facilitate the penetration into heterogeneous media, by minimizing channeling (Bouzid and Fatin-Rouge, 2022; Martel et al., 1998, 2004).

The performance of the injection of the polymer solutions alone or in combination with other chemical compounds in the recovery of pollutants in contaminated soils has been studied (Martel et al., 1998). found that pre-flushing with xanthan improved surfactant (Sodium Alkane Sulfonate) transport in a three-layered, heterogeneous system with varying permeabilities by preventing surfactant adsorption and

controlling surfactant mobility. Robert et al. (2006) conducted a set of multiphase flow experiments in a heterogeneous 2D sandbox, where Trichloroethylene (TCE) was initially distributed in two states; at residual saturation and in pool. They illustrated that the injection of a mixture of xanthan and surfactant could result in 0.90 recovery factor of TCE by minimizing the effect of heterogeneities. They assessed density-driven plume sinking, caused by DNAPL dissolution in a mixture of surfactant and polymer. Density difference and the Darcy velocity magnitude were found to influence downward migration of surfactant polymer mixture containing the dissolved DNAPL. However, the range of density difference between the surfactant mixture and the surrounding groundwater was limited to 0.0045 g/mL. Silva et al. (2013) numerically simulated the transport of xanthan in a previously water saturated stratified sand pack. Their results showed that the injection of xanthan solution in multilayer systems assists the cross-flow between the layers and consequently the displacement efficiency. Bouzid and Fatin-Rouge (2022) through 2D experiments found that by injection of the mixture of xanthan and Sodium dodecyl sulfate (SDS), displacement efficiency could reach up to 0.90. They used a two-layer porous medium with contrasted permeabilities (composed of glass beads) packed over an impermeable layer. Although, the injection of the xanthan and surfactant mixture shows a promising efficiency, they performed their experiments in a confined sandbox resulting in an unrealistic extra recovery factor.

Alamooti et al. (2022) numerically and experimentally investigated the influence of densified polymer suspension injection on the displacement of DNAPL (same type as this study) in a 2D system composed of sand packs with permeability around 180 Darcy. They showed that the densification of polymer solution to match the density of DNAPL thus nullifying the effect of gravity forces could improve the displacement efficiency up to four times. For an unconfined system the residual DNAPL saturation after polymer injection was 0.34 compared to 0.11 for a confined one. Density contrast between invading and defending fluids during horizontal displacement can lead to density-driven (overridden/ underridden) flows. Several studies have investigated density-driven flow in 2D systems for DNAPL remediation purposes (Jawitz et al., 1998; Taylor et al., 2004, 2001; Zhong et al., 2008). Despite the analysis conducted, in this study we examine the density-overridden flow phenomenon in the context of immiscible two-phase flow displacement involving the use of polymers for DNAPL remediation. Furthermore, our investigation focuses on a multilayer system, considering the potential impact of crossflow between the layers, which has not been addressed in the previously mentioned studies. Modeling of multiphase flow in a multilayer system corresponding to the polymer-DNAPL displacement experiments can shed light on the efficiency of polymer injection, considering the aforementioned parameters.

Understanding the interaction between xanthan and surfactant is necessary as it can affect their rheological properties and consequently their performance for remediation of DNAPL polluted soils (Krstonošić et al., 2019). using various techniques including scanning electron microscopic (SEM) imaging, and viscosity measurements investigated the interaction between xanthan and the anionic surfactant SDS and found evidence of both electrostatic and hydrophobic interactions. Moreover, several authors have studied the rheological behavior of xanthan gum in the absence or presence of other additives (Huang and Sorbie, 1992; Krstonošić et al., 2019; Zhong et al., 2013). Omirbekov et al. (2023) used an upscaling method and bulk shear viscosity data to study the polymer solution flow. Krstonošić et al. (2019) investigated the rheological behavior of binary mixtures of xanthan and anionic SDS in various concentrations. They observed that at low SDS concentrations and a fixed xanthan concentration, increasing the surfactant concentration decreased the viscosity to a minimum value, but higher surfactant concentrations led to higher viscosities. However, the rheological behavior of xanthan-SDBS mixtures in bulk and in porous media, their interactions and their application for soil remediation remain

understudied.

This study aims to describe the performance of xanthan solutions with or without SDBS as an anionic surfactant on remediation of heavy chlorinated solvents from multilayer system. A series of rheological measurements was performed on the xanthan solutions and mixtures of xanthan and SDBS. Interfacial tension analysis and SEM imaging were performed to evaluate the interactions between SDBS and xanthan. Several 1D-column experiments were carried out to quantify the apparent viscosity of polymer solutions and to assess their performance on the removal of DNAPL. Injection of polymer solution into a DNAPL-contaminated multilayered system was conducted through a confined 2D tank where the pressure along the layers was monitored. An unconfined 2D tank was used to launch the experiments in an unconfined system where the contaminated zone was blocked by injection of polymer suspension through a horizontal well. The numerical modeling was performed by coupling continuity and generalized Darcy's law. The role of the confinement of polluted layers, density difference, and the cross-sectional flow between the layers during the displacement process was assessed using simulation data.

The specific objectives of this study are (i) evaluation of the role of interactions of xanthan and SDBS on their rheological properties; (ii) comparison of the performances of the injection of xanthan solution alone and mixed with SDBS on the remediation of DNAPL from multilayer systems; (iii) using multiphase flow modeling to evaluate of density-driven flow and crossflow during DNAPL remediation by polymer injection in multilayer systems; (iv) assessment of the applicability of polymer injection for the unconfined DNAPL polluted soil (to mimic the real contaminated site).

2. Materials and methods: experimental and numerical

2.1. Experimental materials

Two particle-size fractions of marble sand (0.2 to 0.3 mm and 0.4 to 0.6 mm equivalent to absolute permeabilities of 35±5 and 105±10 darcy respectively) have been used as the solid phase in 1D column and 2D tank studies. They were sieved and washed by deionized water and dried in an oven at 105 °C. The composition and properties of DNAPL used in this study is mentioned in supplementary materials (Table A-1). The polymer chosen for the displacement of DNAPL is xanthan gum, an anionic water-soluble biopolymer extracted from xanthomas with the chemical formula of $C_{35}H_{49}O_{29}$. SDBS as a biodegradable surfactant used in this study showing a good efficiency in the improvement of DNAPL recovery by reducing the surface tension and not by solubilization (Colombano et al., 2020). Both xanthan and SDBS powders were supplied by Sigma-Aldrich.

To analyze the rheological behavior of the polymer solutions, the rotational rheometer Haake Mars 60 equipped with the cone-plate geometry was used. The interfacial tension (IFT) between the polymer solutions and DNAPL was measured through the drop shape analyzer apparatus (DSA-100, KRUSS). The pendant drop method was used to measure the IFT at ambient temperature (22 ± 1 °C). The TOC Shimadzu device was used to measure the effluent's total organic carbon (TOC) concentration to determine the concentration of the polymer solution. The concentration of the bromide ion as tracer was evaluated using ICS 3000 Thermo-Dionex an ionic chromatography apparatus. The morphological analysis of the dried samples of xanthan or xanthan-SDBS solutions was carried out using an Ultra55 Zeiss scanning electron microscope (SEM) operating at a 5 kV acceleration voltage.

2.2. Column experiments

A series of multiphase and single-phase column experiments were carried out to evaluate the displacement of DNAPL in porous media of two different permeabilities, a analyze the transport of polymer solutions (see the procedure outlined by Alamooti et al. (2022)). Briefly, a

glass column (4 cm internal diameter ×30 cm length) was gradually packed with the dried sand pack while being manually vibrated continuously. Next, CO_2 was injected, which due to its solubility in water allows to avoid trapping of gas bubbles during the water saturation process. Then, degassed deionized water was vertically imbibed through the column for 2 pore volumes (PVs) at a flowrate of 0.1 mL/min. Afterward, the porosity and permeability of the porous media were measured. For the single-phase flow experiments, the polymer solutions or a tracer were introduced into a fully water-saturated sand pack with the flowrate of 1 mL/min and samples were collected from the effluent. For the multiphase flow experiments, DNAPL was initially injected vertically into the fully water-saturated column at a flowrate of 1 mL/min until no water was observed in the effluent. Then, the polymer solutions with a flowrate of 1 mL/min were injected into the DNAPL-saturated columns, and the effluent was collected in 15 mL polypropylene tubes while monitoring the pressure at the inlet and outlet of the column using KELLER PR33X pressure transducers. The quantification of DNAPL recovery was accomplished using volumetric measurement of the effluent samples collected at 15 mL interval thanks to discernible variation in color between the aqueous and DNAPL phases.

2.3. 2D tank experiments

Two separate two-dimensional systems were employed to conduct the multiphase flow studies in the multilayer system shown in Fig. A-1. A confined 2D tank, allowing to measure the pressure along the layers, was used to assess the efficiency of injecting polymer solutions into a multilayer heterogeneous system. Another 2D tank was used to mimic the unconfined conditions encountered in a real polluted site (i.e. field pilot) in a laboratory-scale setting. In this case, the contaminated area is confined with a blocking substance (a densified polymer-suspension, same as the one used in Alamooti et al. (2022)) to occupy the pores and resist against the upward movement of the contaminant/remedial polymer. The blocking substance was injected from a horizontal perforated tube with 0.3 cm internal diameter above the contaminated layers. The size of the unconfined 2D tank was 50 cm length × 30 cm height × 2 cm thickness, while the closed system had dimensions of 15 cm × 10 cm × 2 cm. To facilitate imaging, the fronts of the tanks were made of glass.

Two separate layers, each with a height of 5 cm, were established in both systems. Sand was compacted inside the tank while water was continuously injected from the bottom. Once the two layers were fully saturated by water, the DNAPL was uniformly injected from three ports located in bottom part through the layers with rate of 3 × 0.5 mL/min. In the confined tank, the polymer solutions have been injected from two ports in the left side of the tank with the rate of 2 × 0.5 mL/min, whereas in the unconfined one the polymer solution was injected from the port located in the central bottom of the tank at the rate of 2 mL/min. While in the unconfined system the DNAPL was extracted using Reglo ICC digital peristaltic pump (Ismatec®) from the ports on two sides of the tank at the same rate as the polymer injection rate 2 × 1 mL/min, in the case of the confined 2D tank the DNAPL was produced naturally in the effluent by injection of the polymer, similar to the column tests. In the unconfined system, the horizontal perforated line was set above the contaminated zone to inject the polymer suspension. The schematic of polymer injection in 2D systems is depicted in Figure A-1.

2.4. Error and uncertainty estimations

The multiphase flow experiments in 1D column and 2D tank were duplicated. For rheological analysis the experiments have been triplicated. Error bars are calculated by determining the mean (average) of the data points and the standard deviation. The top of the error bar is located at the mean plus the standard deviation, while the bottom is located at the mean minus the standard deviation.

2.5. Polymer/surfactant solutions

Xanthan gum, widely used in soil remediation, was chosen as a biopolymer exhibiting non-Newtonain behavior in solution form. To avoid fingering (Lenormand et al., 1988), the concentration of xanthan was selected at 0.8 g/mL to provide a stable front for the injection rate of 1 mL/min. The concentration of SDBS used was 1265 mg/L, i.e. 5 times the critical micelle concentration, which results in a very slight solubilization of DNAPL at a level of 40 mg/L (Colombano et al., 2021; Rodrigues et al., 2017), this is while the solubility of DNAPL in aqueous phase without SDBS is around 28 mg/L. This concentration was chosen to ensure that a sufficient amount of surfactant reaches all parts of the porous medium.

2.6. Numerical modeling

The numerical modeling was employed to simulate the displacement of DNAPL in a multilayer system using a polymer solution. As the dissolution of DNAPL even in the presence of surfactant is negligible, the modeling focused on polymer injection, excluding the influence of DNAPL dissolution in the aqueous phase.

2.6.1. Two-phase flow in porous media

The contaminated zone is represented as a uniform and isotropic porous medium made up of natural soil, containing two phases that are incompressible and immiscible (water and DNAPL). The continuity equation of each phase can be expressed as follows (Bear, 2013):

$$\frac{\partial}{\partial t}(\varnothing \rho_i S_i) + \nabla \cdot (\rho_i \boldsymbol{u}_i) = 0 \; with \; i = w, \; nw \tag{1}$$

where the subscripts w represents wetting phase composed of water and polymer and nw denotes non-wetting phase, DNAPL. The porosity is denoted by $\varnothing$ (-), density by ρ_i (kg/m³), saturation by S_i (-), Darcy velocity by $\boldsymbol{u}_i$ (m/s) and the time by t (s). Generalized Darcy's law for two-phase flow in porous media is considered:

$$\boldsymbol{u}_i = -\frac{k \; k_{ri}}{\mu_i}(\nabla p_i - \rho_i \boldsymbol{g}) \tag{2}$$

where k (m²) refers to the scalar absolute permeability of the isotropic porous medium, k_{ri} (-) is the relative permeability for phase i. The viscosity and the pressure of phase i as well as the gravity vector are represented by μ_i (Pa.s), p_i (Pa), and $\boldsymbol{g}$ (m/s²) respectively. The soil is fully saturated by aqueous and non-aqueous phases; therefore, the summation of the saturations of wetting and non-wetting phases is always equal to unity. As a non-Newtonian polymer, xanthan exhibits shear-thinning behavior; therefore, its rheological behavior in porous media is represented by its viscosity as a function of pressure gradient, which is derived from single-phase flow experiments in the columns. The capillary pressure, difference in pressure between the aqueous and non-aqueous phases, as well as relative permeability curves are considered as Brooks and Corey functions (Brooks and Corey, 1964):

$$p_c = p_{th} S_{we}^{\frac{-1}{\lambda}} \tag{3}$$

$$k_{rw} = k_{rw}^{max} S_{we}^{\epsilon_w} \tag{4}$$

$$k_{rnw} = k_{rnw}^{max} S_{nwe}^{\epsilon_{nw}} \tag{5}$$

where p_{th} is the threshold pressure (Pa) and λ is the index of the pore size distribution. k_{rw}^{max} and k_{rnw}^{max} are the maximum relative permeability values (end points) for the wetting and non-wetting phases, respectively. The saturation exponents for the wetting and non-wetting phases are given by ϵ_w and ϵ_{nw}. The effective saturations of wetting and non-wetting phases are denoted by S_{we} (-) and S_{nwe} (-) and can be expressed as:

$$S_{we} = \frac{S_w - S_{wr}}{1 - S_{nwr} - S_{wr}} \qquad (6)$$

$$S_{nwe} = \frac{S_{nw} - S_{nwr}}{1 - S_{nwr} - S_{wr}} \qquad (7)$$

where, S_{wr} (-) and S_{nwr} (-) are the wetting irreducible and non-wetting residual saturations respectively.

2.6.2. Polymer transport model

The equation governing polymer transport in porous media, known as the advection-dispersion equation, can be expressed as (O'Carroll et al., 2013; Tsakiroglou et al., 2018):

$$\underbrace{\frac{\partial(\varnothing S_w c)}{\partial t}}_{\text{Accumulation}} \underbrace{- \nabla \cdot (\varnothing S_w D \cdot \nabla c)}_{\text{Dispersion}} + \underbrace{u_w \cdot \nabla c}_{\text{Advection}} = R_i + \dot{m} \qquad (8)$$

where c is the concentration of the polymer (kg/m^3) and $\boldsymbol{D}$ the dispersion tensor. R_i is the reaction term for the i-component and the source term is denoted by $\dot{m}$. As the xanthan is an anionic polymer, the adsorption on the sand surface is neglected. The principal and cross terms of dispersion tensor can be represented as (Bear, 2013):

$$\boldsymbol{D} = \left(\propto_T |\boldsymbol{U}| + D_{eff}\right)\boldsymbol{I} + \left(\propto_L - \propto_T\right)\frac{U_x U_y}{|\boldsymbol{U}|} \qquad (9)$$

$$D_{eff} = \frac{D_0}{\tau} \qquad (10)$$

where $\boldsymbol{I}$ is the identity matrix, D_{eff} is the effective diffusion coefficient (m^2/s) in porous media, D_0 is the molecular diffusion coefficient (m^2/s), τ is the tortuosity, $\propto_L$ and $\propto_T$ are the longitudinal and transverse dispersivities, respectively.

The molecular diffusion coefficient of xanthan as a polysaccharide can be obtained through (Kono, 2014):

$$D_0 = 8.2 \times 10^{-9} Mw^{-0.49} \qquad (11)$$

where Mw (g.mol^{-1}) is the molecular weight of xanthan.

Eqs. (1), (2), and (8) were coupled to simulate the DNAPL displacement by a polymer solution in a multilayer system in a two-dimensional domain. The simulation domain was discretized by 7289 triangular meshes with a maximum element growth rate of 1.2 and maximum and minimum element sizes of 0.3 cm and 0.00112 cm respectively. The mesh is refined near the injection and production ports with the maximum element size of 0.06 cm to improve the convergence of numerical model. MUMPS (multifrontal massively parallel sparse direct solver) in COMSOL (version 5.6) as a finite element solver was used.

COMSOL Multiphysics ® has been previously used for modeling two-phase flow problems in the context of soil remediation. Its effectiveness in simulating the coupled flow ad transport phenomena in porous media has been successfully demonstrated for both Newtonian (Koohbor et al., 2023) and non-Newtonian fluids (Alamooti et al., 2022; Davarzani et al., 2022). The mesh sensitivity was analyzed based on the phase distribution and recovery factor after 70 min of injection. The results revealed that three different mesh sizes, consisting of 1338, 2142 and 7289 triangular mesh elements, yielded identical phase distribution and recovery factor. Nevertheless, the finest mesh was chosen due to its acceptably low computational time. A backward differentiation formula (BDF) for time stepping approach with the free time stepping option was used allowing to have flexible time-steps needed to meet the specified tolerance (with tolerance factor of 0.1). For 1D column, the inlet boundary condition for DNAPL displacement by the polymer solution was set as a fixed injection velocity of 1 mL/min, while the outlet boundary condition was set as constant atmospheric pressure (Fig. A-2a). For 2D tank case, the constant injection rate of 0.5 mL/min

for the injection ports and the constant atmospheric pressure in the outlet were considered as the boundary conditions (Fig. A-2b).

3. Results and discussion

3.1. Rheological behavior and polymer surfactant interactions

A rotational rheometer (Haake Mars 60) with a shallow angled rotational cone plate (1°) was used to study the rheological behavior of polymer solutions, specifically xanthan solutions with and without SDBS. The results for the rheological behavior of the mixture of xanthan and SDBS solution at fixed xanthan concentration of 800 mg/L and various concentrations of SDBS are presented in Fig. 1. The rheological behavior of pure xanthan solution and mixture of xanthan & surfactant was described through the Carreau fluid model (Carreau, 1972) expressed as:

$$\mu = \mu_{inf} + \left(\mu_0 - \mu_{inf}\right)\left(1 + (\chi\dot{\gamma})^2\right)^{\frac{l-1}{2}} \qquad (12)$$

where, the viscosities (Pa.s) at zero and infinite shear rate are denoted as μ_0 and μ_{inf}, χ is the relaxation time (s), and l (-) is the power index. The fitted curve and parameters of Carreau model are shown in Fig. 1 and Table A-2 respectively.

The results shown in Fig. A-3 depict that by increasing the concentration of pure xanthan solutions, the viscosity also increases, while exhibiting similar shear thinning behavior. As it can be seen in Fig. 1, the addition of surfactant SDBS to a fixed concentration of xanthan solution decreases the viscosity (mainly at low shear rate). It also expands the range of shear rate where the solution exhibits Newtonian behavior (at low shear rates), but there are no significant changes in the rheological behavior as the concentration of SDBS increases. The decrease in viscosity is explained by the shrinkage of the xanthan chains due to the existence of repulsive electrostatic forces between xanthan and SDBS (Yang and Pal, 2020). As the concentration of SDBS increases, the interaction between the hydrophobic parts of xanthan and SDBS counterbalances the repulsive forces, causing no further noticeable changes in the viscosity of the mixture (Krstonošić et al., 2019).

To gain further insight into the interaction between xanthan and SDBS, additional analysis was conducted using scanning electron microscopy (SEM). The microstructures of solutions of pure xanthan, pure SDBS, and their mixture are presented in Fig. 2. The SEM imaging reveals that the hydrophobic interactions between xanthan and SDBS altered the microsctructure of the xanthan gum (Krstonošić et al., 2019).

A series of 1D column experiments were carried out to determine the apparent viscosity of xanthan solutions in the two soils with different permeabilities, with and without the addition of surfactant. The shear rate within porous media at the Darcy scale can be described using the
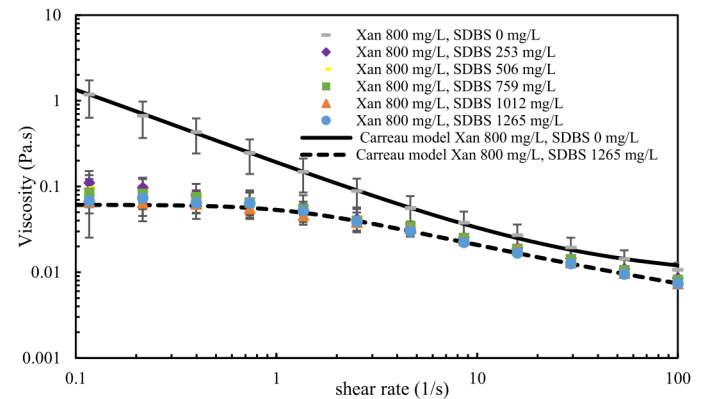

Fig. 1. Rheological behavior of the mixture of xanthan and SDBS solution at fixed xanthan concentration of 800 mg/L and various concentrations of SDBS and Carreau models fitted on experimental data.
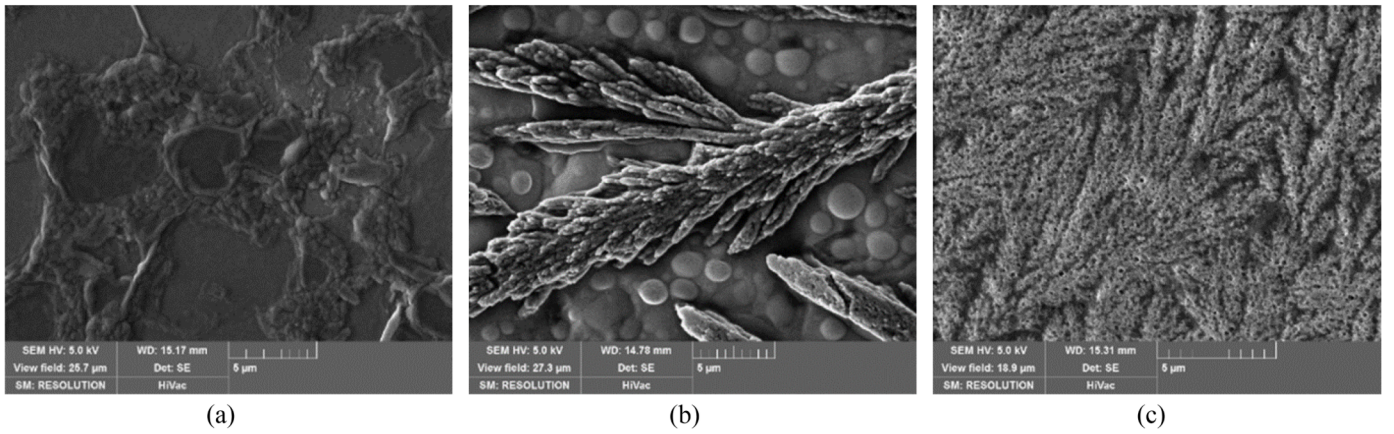
Fig. 2. SEM micrographs. (a) SDBS 1265 mg/L, (b) xanthan 800 mg/L, and (c) mixture of xanthan 800 mg/L and SDBS 1265 mg/L.

Darcy velocity as (Darby et al., 2017):

$$\dot{\gamma} = \sqrt{\frac{2}{\phi k}} \alpha u \tag{13}$$

where, the empirical shifting parameter, α (-), is related to both the tortuosity of the porous media and the fluid's bulk rheology (Chauveteau and Zaitoun, 1981). To determine the shift parameter, the apparent shear rate was calculated by fitting the Carreau fluid model to the apparent viscosity data. Actually, the apparent shear rate is plotted against the normalized Darcy velocity $\frac{u}{\sqrt{k}}$ and a linear curve passing through the origin is fitted to the data. The slope of this curve is considered to be the shift parameter (Zamani et al., 2015). The resulting viscosity curves in porous media compared to those at bulk are shown in Fig. A-4. The shift parameter for the case of mixture of xanthan-SDBS is close to unity showing that the viscosities at bulk and porous media are close, while for the case of xanthan the shift parameter is more than two (2.9 and 2.41 for low and high permeable media, respectively).

The difference in shift factor in different porous media for the xanthan solution can be explained by the depleted layer concept, which describes a concentration gradient that occurs near the pore wall due to steric hindrances. As the xanthan molecules are relatively large, the steric hindrances caused by the pore walls prevent these molecules from coming too close to the wall, resulting in a gradient from zero concentration at the wall to bulk concentration at a distance close to polymer macromolecular half-length (Chauveteau and Zaitoun, 1981).

For the finer sand as the pore size is smaller, the ratio of the thickness of the depleted layer to the pore size becomes larger, and results in a decrease in apparent viscosity vs bulk viscosity and consequently higher shift factor. The depleted layer effect decreases as the shear rate increases, due to the increase in viscous friction in converging zones of porous medium where the polymer molecules are aligned in the direction of flow.

However, when SDBS is present, the mutual presence of the electrostatic repulsion and hydrophobic interactions can cause the xanthan molecule to collapse into a more compact and rod-like shape (Higiro et al., 2007; Rochefort and Middleman, 2000). This results in an alignment of polymer molecules along the direction of flow. This leads to a more uniform distribution of the polymer molecules within the pores, resulting in an increase in the apparent viscosity of the solution. Consequently, the shift factor for the xanthan-SDBS mixture is found to be around unity, implying that there is little or no difference between the bulk viscosity and the apparent viscosity in the porous medium.

3.2. One dimensional displacement

The 1D column experiments were performed to characterize the polymer solutions flow in porous media. This included single-phase and two-phase flow experiments. The single-phase experiments aimed to study the rheological behavior and adsorption/dispersion of polymer solutions in porous media. The results indicate that there is nearly no adsorption of xanthan or SDBS components onto the solid surface, likely due to the repulsive forces between the negative charges on the solid surface and the xanthan/SDBS molecules (Amirmoshiri et al., 2020). The tracer tests and polymer/surfactant injection results are discussed in the supplementary material and the breakthrough curves are shown in Fig. A-5.

The results of 1D column two-phase flow experiments were used to determine relative permeability and capillary pressure curves, through inverse modeling. The xanthan solutions with and without SDBS were injected into the two DNAPL-saturated sand packs and the production data and pressure differences were recorded. The capillary number used to evaluate the performance of DNAPL production during the injection of the polymer solutions was calculated as (Chatzis and Morrow, 1984):

$$N_{ca} = \frac{k \nabla p}{\sigma} \tag{14}$$

where σ (mN/m) is the interfacial tension (IFT) between the DNAPL and solutions. The IFT for the xanthan solution and the mixture of xanthan-SDBS was found around 21.5 ± 0.05 and 1.5 ± 0.05 mN/m, respectively. Fig. 3 presents the recovery factor $\left(\frac{\text{volume of DNAPL produced}}{\text{initial volume of DNAPL in sand}}\right)$ and capillary numbers against the injected PV of polymer solutions in the two sand packs.

The recovery factor curves (Fig. 3a) show that the presence of surfactant in the polymer solution enhances the recovery factor by around 0.15 (from 0.77 to 0.91 for fine sand and 0.79 to 0.95 for coarse sand). Additionally, the xanthan-SDBS mixture results in a longer production period after breakthrough due to the reduced interfacial tension with DNAPL. The breakthroughs for a mixture of xanthan-SDBS and xanthan solution are at 0.65 and 0.47 PV for coarse sand, and at 0.56 and 0.48 PV for fine sand, respectively. The capillary number graphs (Fig. 3b) indicate that the xanthan-SDBS mixture results in a higher capillary number, due to the lower interfacial tension and viscosity leading to a lower differential pressure. The capillary number increases until breakthrough, then remains relatively constant, as the average mobility ratio $\left(\frac{k_{rw}\mu_{nw}}{k_{rnw}\mu_w}\right)$ decreases with the invasion of polymer solutions.

With the aim of modeling the xanthan-DNAPL flow in multilayered system, the saturation functions ($k_{rw}, k_{rnw}, p_c,$) of the invading polymer and DNAPL for each layer have been determined. The model incorporated the continuity equation and generalized Darcy's law, as well as the non-Newtonian properties of the polymer solution, and viscosity data obtained from single-phase flow experiments (as seen in Figure A-6). Using the inverse modeling method the parameters for the relative
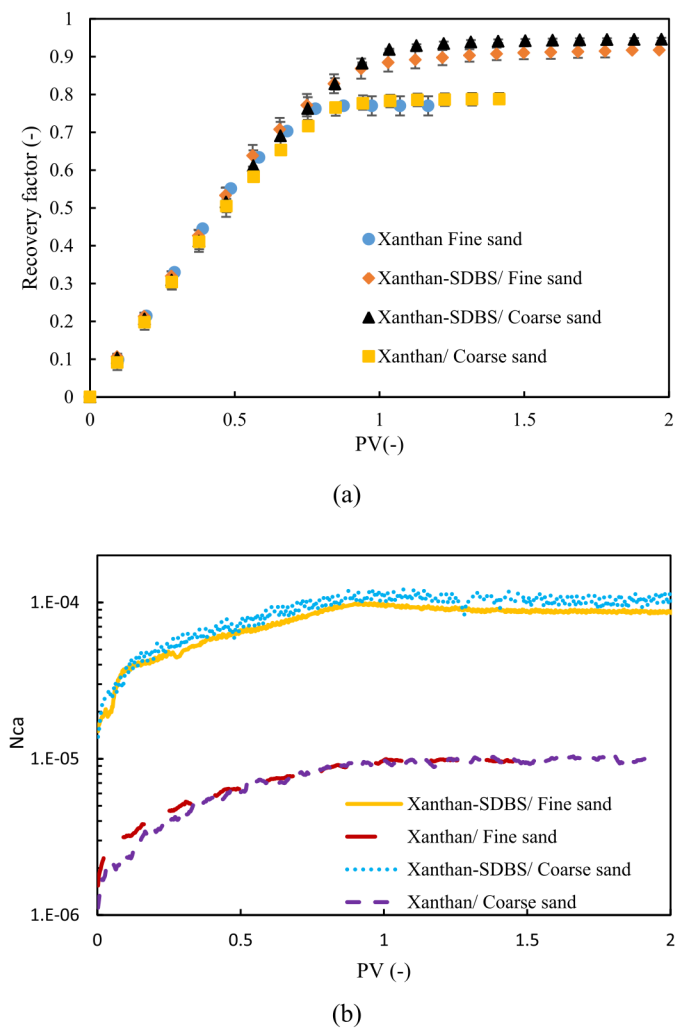
(a)

(b)

Fig. 3. Performance of injection of polymer solutions in two sand packs of different permeabilities. (a) Recovery factor, (b) Capillary number versus injected PV.

permeability and capillary pressure Eqs. (3)–((5) were found. In other words, a mathematical model for two phase flow in porous media, composed of the continuity and the generalized Darcy's law for the two phases and involving the constitutive relationships for relative permeability and capillary pressure is used to simulate two-phase flow. Then, the unknown parameters of relative permeability and capillary pressure curves were adjusted to minimize the mismatch between the model predictions and the experimental data including the differential pressure measurement and the recovery rate.

Figure A-7 displays the matched production and differential pressure data, and the parameters of the saturation functions and mean absolute error between the numerical and experimental data can be found in Table A-3.

3.3. Two-dimensional displacement

Two-dimensional experiments were carried out to study the displacement of DNAPL in a multi-layered system using polymer solutions. A two-phase flow displacement simulation of DNAPL by xanthan solution was also conducted to better understand the mechanisms involved in the displacement process.

3.3.1. DNAPL removal in multi-layer system, xanthan solutions with/without SDBS

In line with two-phase flow experiments in 1D column, the 2D experiments were carried out in a two-layer system by injection of polymer solutions to displace the DNAPL. The polymer solutions were injected through the contaminated layers, following the steps outlined in Section 2.2. Fig. 4 illustrates the distribution of the polymer solutions and DNAPL at different injected PVs. The average residual DNAPL saturation after xanthan-SDBS injection is 0.13 and for xanthan injection is 0.195 which is consistent with the previous experiments in columns. The displacement of DNAPL for both cases of xanthan solution injection and xanthan-SDBS mixture injection was similar; however, the presence of SDBS in the polymer solution resulted in a lower residual saturation. Also in the presence of SDBS in xanthan solution two fronts in the system can be observed which is likely due to the surfactant's ability to reduce IFT and enhance the mobilization of more DNAPL.

The data presented in Figure A-8 highlights the impact of surfactant-polymer mixture on the recovery of dense non-aqueous phase liquid (DNAPL) and the pressure gradient in the layers. The results indicate that the presence of SDBS in the polymer mixture reduces the pressure (~350 Pa for fine sand and ~180 Pa for coarse sand), leading to a higher recovery of DNAPL by 0.07 (0.85 compared to 0.78). The pressure drop is higher in low permeable layer, and the duration of DNAPL production is prolonged after the breakthrough when SDBS is present. The displacement of DNAPL and polymer solutions is influenced not only by the permeability contrast but also by the density difference between the polymer solutions and DNAPL. The invading solution tends to flow on the top of high permeable layers as buoyancy forces favor the vertical movement of the polymer solutions. Indeed, the comparison of dimensionless numbers including capillary and Bond numbers can provide valuable insight into the complex interplay of forces that drive DNAPL displacement by polymer solutions. By evaluating the values of these dimensionless numbers, it is possible to determine the relative influence of gravity, capillary, and viscous forces on the displacement process. The Bond number is defined as (Morrow and Songkran, 1981):

$$N_{Bo} = \frac{\nabla \rho g k}{\sigma} \tag{15}$$

The Bond number to capillary number ratio, evaluated at the end of experiment, for the high permeable layer, is 7.15 and 8.57 for injections of xanthan and xanthan-SDBS, respectively. Meanwhile, for the low permeable layer, the ratio is 3.65 and 4.4 for injections of xanthan and xanthan-SDBS, respectively. This shows that gravity forces are stronger than viscous forces for both layers and polymer solutions with or without surfactant. This demonstrates the significance of gravity forces and how they, along with viscous forces, play an active role in the displacement of DNAPL (Zhou et al., 1994). As a result, the flow in the higher permeable layer is faster, and the density difference leads to a preference for flow on top of the DNAPL zone. For the cases where the permeability contrasts are higher, the displacement of the pollutant in the low permeable layer would have a much larger delay compared to the high permeable layer leading to an uncomplete displacement in the low permeable layer in our experimental conditions.

The simulation of DNAPL displacement in a multilayer system using xanthan solution was performed using the constitutive relationships gathered from 1D column experiments. Fig. 5 shows the close match of saturation profiles obtained numerically and experimentally. The comparison for recovery factor and pressure drop is shown in Fig. A-9. The dynamic of propagation of the front in both layers influenced by gravity and capillary forces has been relatively well captured by numerical model. The simulation results depicts that the recovery factor for high permeable layer is around 0.79 while for low permeable layer it is approximately 0.74. This model is used for further analysis where the role of densification of polymer solution, the boundary conditions and cross-sectional flow along the layers is evaluated.
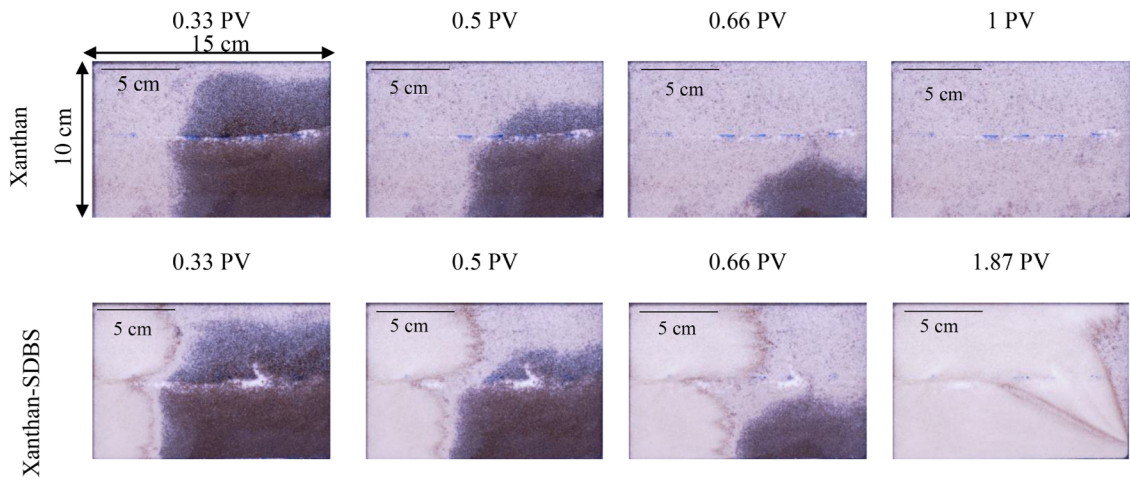
Fig. 4. DNAPL displacement in a 2D multilayer system by injection of xanthan solution (first row) and mixture of xanthan-SDBS (second row) at different pore volumes of injected fluids.
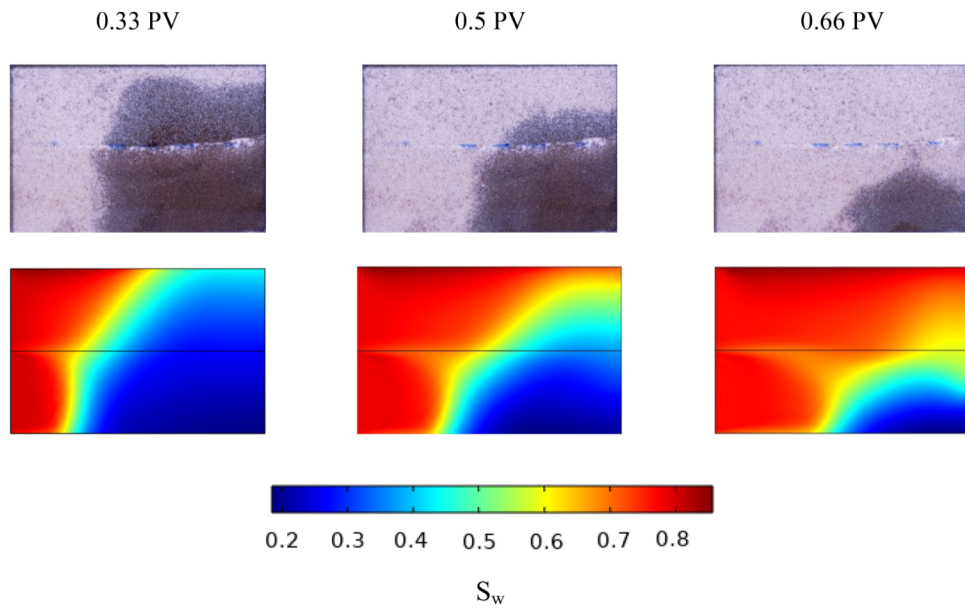

Fig. 5. Comparison between the numerical and experimental results of DNAPL displacement by xanthan solution in a 2D multilayer system, first row: experimental results shown; second row simulation results depicted.
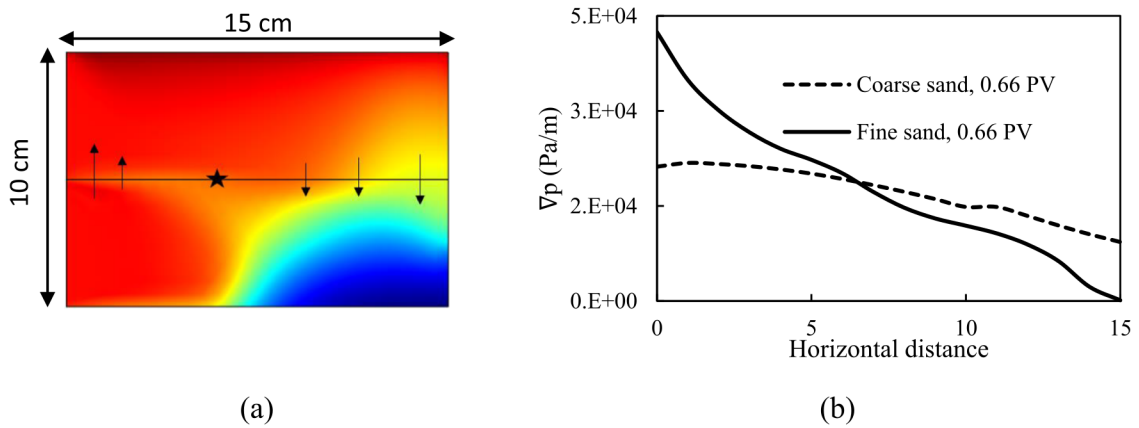

(a)   (b)

Fig. 6. Crossflow between the layers after 0.66 PV injection of xanthan in a 2D multilayer system. (a) xanthan-DNAPL distribution in the system, the arrows show the direction of crossflow and the star shows zero cross flow, (b) pressure gradient along the layers.

3.3.2. Cross sectional flow

Nonuniform fluid flow in porous media can occur due to factors such as permeability heterogeneity, adverse mobility ratio, and differences in density between the injected fluid and the contaminant (Debbabi et al., 2017). This type of flow can lead to fluid crossflow between zones of fast and slow flow in the layers, which may be caused by various mechanisms such as viscous crossflow, capillary crossflow, or density-driven crossflow. According to the simulation data analysis, crossflow between the layers occurs during the displacement of DNAPL. As depicted in Fig. 6, the crossflow direction is from the low permeable layer to the high permeable layer near injection points, decreasing to zero at the middle of the horizontal axis. Near the recovery point, the crossflow direction is reversed. These results align with the pressure gradient profile within the layers, where crossflow direction depends on the pressure gradient difference. Higher pressure gradient leads to crossflow from high to low gradient zones. Zero crossflow occurs at the intersection of pressure gradient curves.

3.3.3. Evaluation of polymer injection performance in an unconfined polluted site

The displacement of DNAPL by a polymer solution in the subsurface is a complex process that is influenced by several factors, including the density contrast between the two fluids. In traditional soil remediation technologies, the polymer solution is usually less dense than the DNAPL, resulting in an upward flow of the DNAPL due to buoyancy forces. However, recent studies have suggested that the densification of the polymer solution can alter the direction and distribution of DNAPL flow through the soil (Alamooti et al., 2022; Omirbekov et al., 2023).

To numerically assess the densification impact on fluid distribution, the density of the invading polymer solution in the soil is modified to match that of DNAPL, which has a density of 1.66 g/mL. Fig. A-10 shows that densification reduces vertical movement of the invading fluid while promoting horizontal flow. However, the permeability contrast between the layers still controls the flow in the layers, with faster flow in high permeable layers and slower flow in low permeable layers. These findings highlight the importance of considering density contrast and densification when designing remediation strategies for DNAPL-contaminated sites. For the case of non-densified polymer injection through the DNAPL-contaminated sites where the polluted zone is not confined and is open to adjacent areas, the upward movement of the polymer can negatively impact the remediation of DNAPL. To evaluate this, a simulation analysis was conducted with the upper boundary of the multilayer system considered as an open boundary with constant atmospheric pressure boundary conditions. The results of the simulation, as shown in Figure A-11, indicate that after one PV of injection, the polymer solution has not reached half of the system and has primarily moved upward. The recovery factor is around 0.38 less than half of the recovery factor in a confined system. This indicates that, in a real field, polymer injection alone is much less effective without densification or blocking of the contaminated zone.

To address this issue in a more realistic manner, a larger 2D tank (as shown in Figure A-1a) was used, where the contaminated zone was blocked by injection of a densified polymer suspension at the same density as DNAPL. The polymer suspension contained carboxymethyl cellulose at a concentration of 4 g/L and added barite particles to achieve a density of 1.66 g/mL (Alamooti et al., 2022). The blocking suspension was continuously injected above the contaminated layers to prevent the vertical movement of invading polymer solution. Fig. 7 demonstrates that in a system similar to a real polluted site, the injection of the blocking agent can effectively improve remediation during the displacement of DNAPL by polymer solution. DNAPL recovery factor in this system has been 0.87.

4. Conclusion

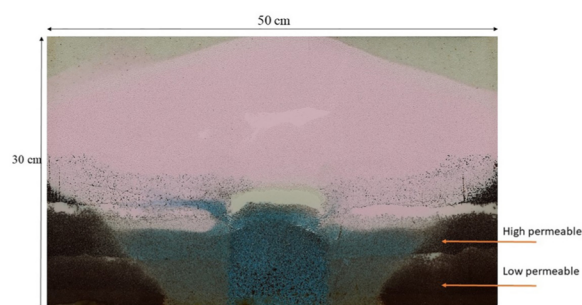Experiments were conducted to assess the performance of the

Fig. 7. DNAPL displacement by xanthan solution (black-blue) in a 2D multilayer system where the contaminated zone is blocked by the injection of a densified polymer suspension (pink) through a horizontal well. (For interpretation of the references to colour in this figure legend, the reader is referred to the web version of this article.)

injection of xanthan solutions with or without SDBS for remediating DNAPL-contaminated layered zones, including rheological analysis in both bulk and porous media and 1D and 2D multiphase flow. A numerical study was also conducted to understand the mechanisms involved in the removal of DNAPL in heterogeneous soil. The presence of SDBS decreased the viscosity of the xanthan solution, while there are no significant changes in the rheological behavior as the concentration of SDBS increases. The repulsive electrostatic forces and hydrophobic interaction between their molecules were responsible for this behavior.

The addition of SDBS to the xanthan solution resulted in a better recovery of DNAPL by increasing the capillary number during the injection of the mixture, with an improvement of approximately 0.15 in a 1D homogeneous system and 0.7 in a 2D layered system. The 2D experiments revealed that the displacement of DNAPL was affected by permeability difference and density contrast.

Simulation results validated by experimental data showed that, if the invading polymer solution was not densified and the soil above the DNAPL was not confined, the recovery of DNAPL was less than half of the confined system (0.35 compared to 0.78). In a larger 2D experimental system, injection of xanthan led to 0.87 recovery of DNAPL when the contaminated layered zones were impeded by a blocking agent, suggesting that for a field application, the combination of injecting a polymer mixture with blocking the contaminated zone can lead to a promising remediation of DNAPL-contaminated layered zones.

Declaration of Competing Interest

The authors declare that they have no known competing financial interests or personal relationships that could have appeared to influence the work reported in this paper.

Data availability

The data that has been used is confidential.

Conte (BRGM) for the TOC and bromide ions analysis.

Supplementary materials

Supplementary material associated with this article can be found, in the online version, at doi:10.1016/j.watres.2023.120305.

References

Alamooti, A., Colombano, S., Omirbekov, S., Ahmadi, A., Lion, F., Davarzani, H., 2022. Influence of the injection of densified polymer suspension on the efficiency of DNAPL displacement in contaminated saturated soils. J. Hazard. Mater. 440, 129702 https://doi.org/10.1016/j.jhazmat.2022.129702.

Amirmoshiri, M., Zhang, L., Puerto, M.C., Tewari, R.D., Bahrim, R.Z.B.K., Farajzadeh, R., Hirasaki, G.J., Biswal, S.L., 2020. Role of wettability on the adsorption of an anionic surfactant on sandstone cores. Langmuir 36, 10725–10738. https://doi.org/10.1021/acs.langmuir.0c01521.

Bear, J., 2013. Dynamics of Fluids in Porous Media.

Bouzid, I., Fatin-Rouge, N., 2022. Assessment of shear-thinning fluids and strategies for enhanced in situ removal of heavy chlorinated compounds-DNAPLs in an anisotropic aquifer. J. Hazard. Mater. 432, 128703 https://doi.org/10.1016/j.jhazmat.2022.128703.

Brooks, R.H., Corey, A.T., 1964. Hydraulic properties of porous media and their relation to drainage design. Trans. ASAE 7, 26–28.

Carreau, P.J., 1972. Rheological equations from molecular network theories. Trans. Soc. Rheol. 16, 99–127. https://doi.org/10.1122/1.549276.

Chatzis, I., Morrow, N.R., 1984. Correlation of capillary number relationships for sandstone. Soc. Petrol. Eng. J. 24, 555–562. https://doi.org/10.2118/10114-PA.

Chauveteau, G., Zaitoun, A., 1981. Basic rheological behavior of xanthan polysaccharide solutions in porous media: effects of pore size and polymer concentration. In: Proceedings of the First European Symposium on Enhanced Oil Recovery. Society of Petroleum Engineers, Bournemouth, England, pp. 197–212. Richardson, TX.

Colombano, S., Davarzani, H., van Hullebusch, E.D., Huguenot, D., Guyonnet, D., Deparis, J., Ignatiadis, I., 2020. Thermal and chemical enhanced recovery of heavy chlorinated organic compounds in saturated porous media: 1D cell drainage-imbibition experiments. Sci. Total Environ. 706, 135758 https://doi.org/10.1016/j.scitotenv.2019.135758.

Colombano, S., Davarzani, H., van Hullebusch, E.D., Huguenot, D., Guyonnet, D., Deparis, J., Lion, F., Ignatiadis, I., 2021. Comparison of thermal and chemical enhanced recovery of DNAPL in saturated porous media: 2D tank pumping experiments and two-phase flow modelling. Sci. Total Environ. 760, 143958 https://doi.org/10.1016/j.scitotenv.2020.143958.

Darby, Ronald, Darby, Ron, Chhabra, R.P., 2017. Chemical Engineering Fluid Mechanics, Revised and Expanded. CRC Press. https://doi.org/10.1201/9781315274492.

Davarzani, H., Aranda, R., Colombano, S., Laurent, F., Bertin, H., 2022. Modeling and monitoring of foam propagation in highly permeable porous media under lateral water flow. Adv. Water Resour. 166, 104225 https://doi.org/10.1016/J.ADVWATRES.2022.104225.

Debbabi, Y., Jackson, M.D., Hampson, G.J., Fitch, P.J.R., Salinas, P., 2017. Viscous crossflow in layered porous media. Transp. Porous Media 117, 281–309. https://doi.org/10.1007/s11242-017-0834-z.

Higiro, J., Herald, T.J., Alavi, S., Bean, S., 2007. Rheological study of xanthan and locust bean gum interaction in dilute solution: effect of salt. Food Res. Int. 40, 435–447. https://doi.org/10.1016/J.FOODRES.2006.02.002.

Huang, Y., Sorbie, K.S., 1992. The Adsorption and in-situ rheological behavior of xanthan solution flowing through porous media. In: in: SPE/DOE Enhanced Oil Recovery Symposium. OnePetro. https://doi.org/10.2118/24153-MS.

Jawitz, J.W., Annable, M.D., Rao, P.S.C., 1998. Miscible fluid displacement stability in unconfined porous media:: Two-dimensional flow experiments and simulations. J. Contam. Hydrol. 31, 211–230. https://doi.org/10.1016/S0169-7722(97)00062-4.

Kono, H., 2014. Characterization and properties of carboxymethyl cellulose hydrogels crosslinked by polyethylene glycol. Carbohydr. Polym. 106, 84–93. https://doi.org/10.1016/j.carbpol.2014.02.020.

Koohbor, B., Colombano, S., Harrouet, T., Deparis, J., Lion, F., Davarzani, D., Ataie-Ashtiani, B., 2023. The effects of water table fluctuation on LNAPL deposit in highly permeable porous media: a coupled numerical and experimental study. J. Contam. Hydrol. 256, 104183

Krstonošić, V., Milanović, M., Dokić, L., 2019. Application of different techniques in the determination of xanthan gum-SDS and xanthan gum-Tween 80 interaction. Food Hydrocoll. 87, 108–118. https://doi.org/10.1016/S0169-7722(97)00062-4.

Lee, M., Kang, H., Do, W., 2005. Application of nonionic surfactant-enhanced in situ flushing to a diesel contaminated site. Water Res. 39, 139–146. https://doi.org/10.1016/j.watres.2004.09.012.

Lenormand, R., Touboul, E., Zarcone, C., 1988. Numerical models and experiments on immiscible displacements in porous media. J. Fluid Mech. 189, 165–187. https://doi.org/10.1017/S0022112088000953.

Liao, S., Saleeba, Z., Bryant, J.D., Abriola, L.M., Pennell, K.D., 2021. Influence of aqueous film forming foams on the solubility and mobilization of non-aqueous phase liquid contaminants in quartz sands. Water Res. 195, 116975 https://doi.org/10.1016/j.watres.2021.116975.

Martel, K.E., Martel, R., Lefebvre, R., Gélinas, P.J., 1998. Laboratory study of polymer solutions used for mobility control during in situ NAPL recovery. Ground Water Monit. Remediat. 18, 103–113. https://doi.org/10.1111/j.1745-6592.1998.tb00734.x.

Martel, R., Hébert, A., Lefebvre, R., Gélinas, P., Gabriel, U., 2004. Displacement and sweep efficiencies in a DNAPL recovery test using micellar and polymer solutions injected in a five-spot pattern. J. Contam. Hydrol. 75, 1–29. https://doi.org/10.1016/j.jconhyd.2004.03.007.

Morrow, N.R., Songkran, B., 1981. Effect of Viscous and Buoyancy Forces on Nonwetting Phase Trapping in Porous media, Surface phenomena in Enhanced Oil Recovery. Springer. https://doi.org/10.1007/978-1-4757-0337-5_19.

O'Carroll, D., Sleep, B., Krol, M., Boparai, H., Kocur, C., 2013. Nanoscale zero valent iron and bimetallic particles for contaminated site remediation. Adv. Water Resour. 51, 104–122. https://doi.org/10.1016/J.ADVWATRES.2012.02.005.

Omirbekov, S., Colombano, S., Alamooti, A., Batikh, A., Cochennec, M., Amanbek, Y., Ahmadi-Senichault, A., Davarzani, H., 2023. Experimental study of DNAPL displacement by a new densified polymer solution and upscaling problems of aqueous polymer flow in porous media. J. Contam. Hydrol. 252, 104120 https://doi.org/10.1016/j.jconhyd.2022.104120.

Omirbekov, S., Davarzani, H., Ahmadi-Senichault, A., 2020. Experimental study of non-newtonian behavior of foam flow in highly permeable porous media. Ind. Eng. Chem. Res. 59, 12568–12579. https://doi.org/10.1021/acs.iecr.0c00879.

Pennell, K.D., Abriola, L.M., 2017. Surfactant-enhanced aquifer remediation: fundamental processes and practical applications. Fundamentals and Applications. Routledge, pp. 693–750.

Robert, T., Martel, R., Conrad, S.H., Lefebvre, R., Gabriel, U., 2006. Visualization of TCE recovery mechanisms using surfactant-polymer solutions in a two-dimensional heterogeneous sand model. J. Contam. Hydrol. 86, 3–31. https://doi.org/10.1016/j.jconhyd.2006.02.013.

Rochefort, W.E., Middleman, S., 2000. Rheology of xanthan gum: salt, temperature, and strain effects in oscillatory and steady shear experiments. J. Rheol. (N. Y. N.Y.) 31, 337. https://doi.org/10.1122/1.549953.

Rodrigues, R., Betelu, S., Colombano, S., Masselot, G., Tzedakis, T., Ignatiadis, I., 2017. Influence of temperature and surfactants on the solubilization of hexachlorobutadiene and hexachloroethane. J. Chem. Eng. Data 62, 3252–3260. https://doi.org/10.1021/acs.jced.7b00320.

Silva, J.A.K., Liberatore, M., Mccray, J.E., Asce, M., 2013. Characterization of Bulk Fluid and Transport Properties for Simulating Polymer-Improved Aquifer Remediation. https://doi.org/10.1061/(ASCE)EE.1943-7870.0000616.

Taylor, T.P., Pennell, K.D., Abriola, L.M., Dane, J.H., 2001. Surfactant enhanced recovery of tetrachloroethylene from a porous medium containing low permeability lenses: 1. Experimental studies. J. Contam. Hydrol. 48, 325–350. https://doi.org/10.1016/S0169-7722(00)00185-6.

Taylor, T.P., Rathfelder, K.M., Pennell, K.D., Abriola, L.M., 2004. Effects of ethanol addition on micellar solubilization and plume migration during surfactant enhanced recovery of tetrachloroethene. J. Contam. Hydrol. 69, 73–99. https://doi.org/10.1016/S0169-7722(03)00151-7.

Tsakiroglou, C.D., Sikinioti-Lock, A., Terzi, K., Theodoropoulou, M., 2018. A numerical model to simulate the NAPL source zone remediation by injecting zero-valent iron nanoparticles. Chem. Eng. Sci. 192, 391–413. https://doi.org/10.1016/J.CES.2018.07.037.

Walker, D.I., Cápiro, N.L., Chen, E., Anderson, K., Pennell, K.D., 2022. Micellar solubilization of binary organic liquid mixtures for surfactant enhanced aquifer remediation. J. Surfact. Deterg. 26, 357–368.

Yang, J., Pal, R., 2020. Investigation of surfactant-polymer interactions using rheology and surface tension measurements. Polymers 12, 2302. https://doi.org/10.3390/POLYM12102302. Page12, 2302.

Zamani, N., Bondino, I., Kaufmann, R., Skauge, A., 2015. Effect of porous media properties on the onset of polymer extensional viscosity. J. Pet. Sci. Eng. 133, 483–495. https://doi.org/10.1016/j.petrol.2015.06.025.

Zhong, L., Oostrom, M., Truex, M.J., Vermeul, V.R., Szecsody, J.E., 2013. Rheological behavior of xanthan gum solution related to shear thinning fluid delivery for subsurface remediation. J. Hazard. Mater. 244-245, 160–170. https://doi.org/10.1016/J.JHAZMAT.2012.11.028.

Zhong, L., Oostrom, M., Wietsma, T.W., Covert, M.A., 2008. Enhanced remedial amendment delivery through fluid viscosity modifications: experiments and numerical simulations. J. Contam. Hydrol. 101, 29–41. https://doi.org/10.1016/j.jconhyd.2008.07.007.

Zhou, D., Fayers, F.J., Orr, F.M., 1994. Scaling of multiphase flow in simple heterogeneous porous media. In: SPE/DOE Improved Oil Recovery Symposium. OnePetro. https://doi.org/10.2118/27833-MS.